Article:

Van der Baan, M. and Kendall, J.M. (2002) Estimating anisotropy parameters and traveltimes in the tau-p domain. Geophysics, 67 (4). pp. 1076-1086. ISSN 0016-8033

https://doi.org/10.1190/1.1500368

GEOPHYSICS, VOL. 67, NO. 4 (JULY–AUGUST 2002); P. 1076–1086, 4 FIGS., 4 TABLES.
10.1190/1.1500368

Estimating anisotropy parameters and traveltimes in the τ-p domain

Mirko van der Baan and J. Michael Kendall

ABSTRACT

The presence of anisotropy influences many aspects of seismic wave propagation and has therefore implications for conventional processing schemes. To estimate the anisotropy, we need both forward modelling and inversion tools. Exact forward modelling in anisotropic media is generally done by raytracing. However, we present a new and fast method, using the τ-p transform, to calculate exact P and SV reflection moveout curves in stratified, laterally homogeneous, anisotropic media which requires no ray tracing. Results are exact even if the SV-waves display cusps. In addition, we show how the same method can be used for parameter estimation.

Since inversion for anisotropic parameters is very nonunique, we develop expressions requiring only a reduced number of parameters. Nevertheless, predictions using these expressions are more accurate than Taylor series expansions and are also able to handle cusps in the SV traveltime curves. In addition, layer stripping is a linear process. Therefore, both effective (average) and local (interval) estimates can be obtained.

INTRODUCTION

Anisotropy influences many aspects of seismic wave propagation and its presence may have profound implications for conventional data processing schemes in exploration seismics. One such aspect is the observed moveout of reflections in laterally homogeneous stratified media. Moveout is normally assumed to be hyperbolic, but the presence of anisotropy can introduce significant perturbations, thereby effectively reducing stack quality. Another aspect is accurate time-to-depth conversion; namely, anisotropy leads to differences between theoretical root-mean-square velocities and those derived from stacks and well logs (Banik, 1984; Thomsen, 1986). This phenomenon explains in part the observed difference between NMO velocity estimates derived from conventional stacking analyses and vertical velocities directly estimated from well logs. Furthermore, these discrepancies also explain mis-ties between observed and predicted depths in the presence of anisotropy, thereby pointing to an important industrial problem, especially if diverted wells are to be drilled (Banik, 1984).

A popular approach for estimating anisotropy consists of applying a three-term Taylor series approximation to the reflection moveout curve (e.g., Hake et al., 1984; Tsvankin and Thomsen, 1994). However, even for P-waves, this approach is not exact (Grechka and Tsvankin, 1998). Moreover, moveout curves of SV-waves are only at best accurately described for short offsets (i.e., up to the first kink or cusp on the wave surface). For certain anisotropy models with a vertical symmetry axis (VTI), even the short offsets of SV-waves cannot be handled (Berge, 1991; Tsvankin and Thomsen, 1994). Finally, inversion results for deeper layers heavily depend on the parameters obtained for shallower layers, thus affecting the resolution of deeper structures (Grechka and Tsvankin, 1998).

In this paper, we present a new method for calculating exact reflection moveout curves of stratified, laterally homogeneous, anisotropic media using the τ-p transform. This is done without taking any recourse to ray tracing, which is the conventional tool for computing exact traveltimes in anisotropic media. In addition, we show that inversion procedures are greatly simplified in the τ-p domain. We concentrate on the so-called VTI media (hexagonal symmetry or transverse isotropy with a vertical symmetry axis). However, the method is directly applicable to all media displaying a horizontal symmetry plane (like HTI, i.e., transverse isotropy with a horizontal symmetry axis, and orthorhombic media with a symmetry axis parallel to the z-axis). Moreover, our method is easily generalised to more complicated anisotropy systems (e.g., those with tilted symmetry axes).

Estimating anisotropy parameters in the τ-p domain is not a new idea. It is routinely applied in multi-offset vertical seismic profiles (VSPs) (e.g., walkaways). Local estimates of horizontal and vertical slownesses can be obtained for each source-receiver combination by computing the differential moveout between sources for a fixed receiver and vice versa. In a lateral

Published on Geophysics Online February 19, 2002. Manuscript received by the Editor October 13, 2000; revised manuscript received November 1, 2001.
*University of Leeds, School of Earth Sciences, Leeds LS2 9JT, United Kingdom. E-mail: mvdbaan@earth.leeds.ac.uk; kendall@earth.leeds.ac.uk.

homogeneous earth, these estimates can then be combined to yield the complete phase slowness surface at each depth, thereby allowing for an estimation of the anisotropy parameters with depth (Gaiser, 1990).

Alternatively, Hake (1986) showed that the shape of the moveout curves in the τ-p domain is also closely related to the slowness surface of each layer. Namely, the intercept time τ is a summation over the products of layer thicknesses and vertical slownesses. Since depth is known in a VSP experiment, τ-p transforming the data recorded at each receiver results again in the slowness surfaces which can be interpreted in terms of layer velocities and anisotropy parameters. This can be done by explicitly describing the form of the $\tau(p)$ curves following the approach of Hake (1986), or by assuming that the curves are locally elliptic and inverting separately for small (near-offset) and large (far-offset) values of the horizontal slowness (Schmitt and Kebaili, 1993; Kebaili and Schmitt, 1996).

For surface seismics, the depth of each individual layer is not a priori known. We circumvent this inconvenience however by expressing the $\tau(p)$ curves in terms of their zero-offset arrival times—analogous to the Taylor-series method. Advantages of the τ-p method are that both P- and SV-waves can be handled (even if the latter display cusps) and that a linear layer-stripping procedure is easily implemented. The method, therefore, provides both effective (average) and local (interval) estimates of the anisotropy parameters. The latter are crucial if anisotropy parameters are to be used as a lithology indicator (Winterstein, 1986).

First, we review the theory to predict normal moveout curves using Taylor series expansions. We then describe how the τ-p transform produces the exact reflection moveout curves and what approximations are made to reduce the number of parameters for inversion purposes. Finally, we compare the accuracy of traveltime curves produced by the Taylor series expansion and those resulting from our reduced-parameter expressions by means of synthetic examples using media with elastic coefficients of real shales.

TAYLOR SERIES EXPANSIONS

The most straightforward approximation for reflection moveouts comes from the Taylor series expansion of the $t^2(x^2)$ curve near $x^2 = 0$. That is,

$$t^2(x^2) = A_0 + A_2 x^2 + A_4 x^4 + \cdots \tag{1}$$

with

$$A_0 = t_0^2, \quad A_2 = \left.\frac{d(t^2)}{d(x^2)}\right|_{x=0}, \quad A_4 = \frac{1}{2}\frac{d}{d(x^2)}\left(\frac{d(t^2)}{d(x^2)}\right)\bigg|_{x=0}, \tag{2}$$

where t_0 is the true two-way zero-offset arrival time (Taner and Koehler, 1969; Hake et al., 1984; Tsvankin and Thomsen, 1994). The higher order terms (A_4 and up) describe nonhyperbolic moveout for larger offsets due to the presence of anisotropy and/or vertical heterogeneities.

The short-spread reflection moveouts (i.e., $x/z \le 1$ with x offset and z the reflector depth) are accurately described using the first two terms only. The second coefficient of equation (1), A_2, is equal to the reciprocal of the squared stack velocity v_{nmo}. That is, $A_2 = v_{nmo}^{-2}$. For a homogeneous (one-layer) VTI-medium, v_{nmo}^2 equals

$$\begin{aligned} \alpha_n^2 &= \alpha_0^2(1 + 2\delta), \\ \beta_n^2 &= \beta_0^2(1 + 2\sigma), \end{aligned} \tag{3}$$

for P- and SV-waves, respectively (Thomsen, 1986). The terms α_0 and β_0 represent the vertical P and SV velocities, and $\sigma = (\varepsilon - \delta)\alpha_0^2/\beta_0^2$, with δ and ε the so-called Thomsen parameters (Thomsen, 1986). Banik (1987) gives a physical interpretation of these parameters.

The third coefficient of equation (1), A_4, is expressed as

$$\begin{aligned} A_{4,p} &= -\frac{2(\varepsilon - \delta)}{t_{p,0}^2\alpha_0^4}\frac{1 + 2\delta/f}{(1 + 2\delta)^4}, \\ A_{4,sv} &= \frac{2\sigma}{t_{sv,0}^2\beta_0^4}\frac{1 + 2\delta/f}{(1 + 2\sigma)^4}, \end{aligned} \tag{4}$$

with $f = 1 - \beta_0^2/\alpha_0^2$ (Tsvankin and Thomsen, 1994). Reflection moveout of SH-waves is always purely hyperbolic in VTI media. Therefore, we do not consider this phase in this paper. For P- and SV-waves in VTI media, hyperbolic moveout only occurs in isotropic or elliptically anisotropic media (i.e., $\delta = \varepsilon$ and $\sigma = 0$).

Unfortunately, for long spreads ($x/z \ge 2$), the three-term Taylor series expansion is not accurate because the moveout velocity of the traveltime curves does not converge to the horizontal velocity. Hence, Tsvankin and Thomsen (1994) proposed replacing A_4 by A_4', given by

$$A_4' = \frac{A_4}{1 + Ax^2} \quad \text{with} \quad A = \frac{A_4}{v_{hor}^{-2} - A_2}. \tag{5}$$

Alkhalifah and Tsvankin (1995) showed that, for P-wave moveout, there exists a range of kinematically equivalent models which are governed by the stacking velocity α_n and the parameter η given by

$$\eta \equiv \frac{1}{2}\left(\frac{v_{hor}^2}{v_{nmo}^2} - 1\right) = \frac{\varepsilon - \delta}{1 + 2\delta}. \tag{6}$$

For P-waves, equation (1) now becomes

$$t_p^2(x) = t_{p,0}^2 + \frac{x^2}{\alpha_n^2} - \frac{2\eta x^4}{\alpha_n^2\left[t_{p,0}^2\alpha_n^2 + (1 + 2\eta)x^2\right]}. \tag{7}$$

The multiplication term $(1 + 2\delta/f)/(1 + 2\delta)$ is ignored to derive equation (7). This corresponds to assuming that either $\beta_0 = 0$ or, more sensibly, that the primary influence of δ is already absorbed in η.

In the case of SV-waves, the long-spread moveout cannot be accurately described if kinks or, worse, cusps exist on the wave surface, which happens for $\sigma \ne 0$. Thus, replacing $A_{4,sv}$ by $A_{4,sv}'$ does not result in a higher accuracy (Tsvankin and Thomsen, 1994). Nevertheless, a two-parameter approximation can again be obtained by neglecting $2\delta/f$ in equation (4), which results in

$$t_{sv}^2(x) = t_{sv,0}^2 + \frac{x^2}{\beta_n^2} + \frac{2\sigma x^4}{t_{sv,0}^2\beta_n^4(1 + 2\sigma)^2}. \tag{8}$$

In regions before the kink/cusp, this does not affect accuracy either unless $|\delta|$ is very large.

In the case of multiple layers, the stack velocity, $v^2_{nmo,eff}$, is given by

$$v^2_{nmo,eff} = \frac{1}{t_0}\sum_{i=1}^{N} v^2_{nmo,i}\Delta t_i, \qquad (9)$$

with Δt_i the two-way zero-offset traveltime in layer i, and $v_{nmo,i}$ the interval NMO velocity (Hake et al., 1984). The parameter η in equation (7) is replaced by an effective value,

$$\eta_{eff} = \frac{1}{8}\left\{\frac{1}{\alpha^2_{n,eff}t_{p,0}}\left[\sum_{i=1}^{N}\alpha^2_{n,i}(1+8\eta_i)\Delta t_i\right]-1\right\}, \qquad (10)$$

with $\alpha_{n,i}$, η_i, and Δt_i interval values in layer i (Alkhalifah, 1997; Grechka and Tsvankin, 1998). Similarly, for SV-waves, $A^{(sv)}_{4,eff}$ is now given by

$$A^{(sv)}_{4,eff} = \frac{\left(\sum_i\beta^2_{n,i}\Delta t_i\right)^2 - t_0\sum_i\beta^4_{n,i}\Delta t_i}{4\left(\sum_i\beta^2_{n,i}\Delta t_i\right)^4} + \frac{t_0\sum_i A^{(sv)}_{4,i}\beta^8_{n,i}\Delta t^3_i}{\left(\sum_i\beta^2_{n,i}\Delta t_i\right)^4}, \qquad (11)$$

where $A^{(sv)}_{4,i}$ represents the quartic coefficient for each individual layer, and $\beta_{n,i}$ is the interval stacking velocity for SV-waves given by equation (3) (Tsvankin and Thomsen, 1994).

In the next section, we develop expressions for moveout in the τ-p domain. To facilitate comparison, we need the horizontal slowness p_x for both P- and SV-waves at a particular offset x. Since the horizontal slowness is defined as the differential moveout, it follows from equations (7) and (8) that

$$p^{(p)}_x = \frac{dt_p}{dx} = \frac{x\left(t^4_{p,0}\alpha^4_n + 2t^2_{p,0}\alpha^2_n x^2 + (1+2\eta)x^4\right)}{t_p\alpha^2_n\left(t^2_{p,0}\alpha^2_n + (1+2\eta)x^2\right)^2} \qquad (12)$$

for P-waves and

$$p^{(sv)}_x = \frac{dt_{sv}}{dx} = \frac{x}{t_{sv}\beta^2_n}\left[1+2x^2\beta^2_n A_{4,sv}\right] \qquad (13)$$

for SV-waves. In the case of multiple layers, we are naturally dealing with the effective parameters (9–11) in equations (12) and (13).

PHASE VELOCITIES, TRAVELTIMES, AND THE SLANT STACK

Slant stack

An underlying assumption in deriving the approximate Taylor series coefficients A_2 and A_4 is that group velocities may be approximated with the expressions for the phase velocities (although evaluated at different angles). Hence, the anisotropy is assumed to be weak (Tsvankin and Thomsen, 1994). Unfortunately, phase and group velocities do not coincide (except in symmetry planes); they differ both in magnitude and direction (Musgrave, 1970). However, the mathematical expression relating the group to the phase velocities is rather awkward (Musgrave, 1970; Thomsen, 1986), hence the need to approximate the group velocities using the phase velocities.

To circumvent this problem, a plane-wave decomposition such as the slant stack (also known as the τ-p or Radon transform) can be applied to the data (Hake, 1986). In this case, the data are transformed to the slowness domain, and phase velocities are directly extracted as a function of the horizontal slowness. The advantage of using the phase velocity is that it is the natural velocity to work with in anisotropic media and that exact expressions exist for VTI, HTI, and even orthorhombic media [see, for example, Tsvankin (1997)].

The τ-p transform extracts the phase slownesses since the component of the group velocity vector $\mathbf{v_g}$ parallel to the normal of the plane wave equals the phase velocity. That is,

$$\mathbf{v_g}\cdot\mathbf{p} = 1, \qquad (14)$$

where $\mathbf{p}$ represents the phase slowness vector (Vlaar, 1968). Furthermore, the length and direction of a ray element, as expressed by the vector $\mathbf{l}$, are obtained by rescaling the local group velocity vector with the traveltime t,

$$\mathbf{l} = t\mathbf{v_g}. \qquad (15)$$

And from equation (14),

$$t = \mathbf{p}\cdot\mathbf{l}. \qquad (16)$$

If the analysed plane wave is purely traveling in the x-z plane in a homogeneous medium, equation (16) can be decomposed as

$$t = p_x x + 2p_z z \qquad (17)$$

for a wave reflected at depth z, with p_z the vertical slowness. The second term $2p_z z$ is the intercept time τ and, thus, equation (17) yields the τ-p transform,

$$t = p_x x + \tau. \qquad (18)$$

Alternatively, equation (17) can be derived by realizing that traveltimes of plane waves in homogeneous media can be written as

$$t = \frac{\partial t}{\partial x}x + 2\frac{\partial t}{\partial z}z = p_x x + 2p_z z. \qquad (19)$$

This linear decomposition is exact since p_x and p_z are constant in homogeneous media for a given angle of incidence (Vlaar, 1968).

For an anisotropic earth composed of a stack of horizontal layers, equation (17) can be generalised to

$$t = p_x x + \sum_i z_i(\grave{p}_{z,i} + \acute{p}_{z,i}) \qquad (20)$$

in which z_i represents the thickness of layer i, and $\grave{p}_{z,i}$ and $\acute{p}_{z,i}$ the absolute vertical slowness of, respectively, the down- and upgoing plane waves in that layer (Hake, 1986). Snell's law, which states that the horizontal component p_x of the slowness remains constant for all layers, was used to obtain this expression.

Again, the second term in the right-hand side of equation (20) equals the intercept time τ in equation (18). Moreover, for anisotropic media with a horizontal symmetry plane (like VTI and HTI media), $\grave{p}_{z,i} = \acute{p}_{z,i} = p_{z,i}$. Therefore, equation (20) shows that the total intercept time τ is composed of a summation over all contributing layers. That is,

$$\tau = 2\sum_i z_i p_{z,i} = \sum_i \Delta\tau_i. \qquad (21)$$

Schultz (1982) showed for isotropic media that this particular feature can be used in a layer-stripping procedure to isolate the effect of each single layer, thereby producing an inversion method capable of retrieving the local velocity. This layer-stripping operation remains valid in anisotropic media composed of homogeneous layers (Hake, 1986).

Forward modelling: Exact traveltimes

In order to obtain an expression for τ valid for anisotropic media, we use the fact that $p_{z,i}^2 = v_{ph,i}^{-2} - p_x^2$. This, in combination with equation (21), gives

$$\Delta\tau_i^2 / \Delta\tau_{0,i}^2 = \frac{(2z_i p_{z,i})^2}{(2z_i/v_{0,i})^2} = \frac{v_{0,i}^2}{v_{ph,i}^2}\left[1 - p_x^2 v_{ph,i}^2\right], \tag{22}$$

with $v_{ph,i}$ the phase velocity in layer i, $\Delta\tau_{0,i}$ the two-way interval zero-offset traveltime which equals the interval intercept time of the vertically travelling wave, and $v_{0,i}$ its associated phase velocity.

Formula (22) describes the moveout curves in the τ-p domain. For instance, in homogeneous isotropic media, the hyperbolic reflection moveouts in the x-t domain are transformed to ellipses in the τ-p domain since the phase velocity remains constant everywhere. For anisotropic media, the reflection moveouts no longer map onto perfect ellipses unless the medium is elliptically anisotropic. Nonetheless, equation (22) accurately describes the nonelliptical curves for anisotropy models displaying a horizontal symmetry plane if the phase velocity as function of the horizontal slowness, $v_{ph}(p_x)$, is known.

Expression (22) also describes the form of the $\tau(p_x)$ curves of direct waves recorded in a VSP geometry with the difference that the curves should be normalised with the one-way interval zero-offset times. Furthermore, the factor 2 disappears in equations (17) and (19). Therefore, the methodology described hereafter can directly be applied to the estimation of traveltimes and anisotropy parameters in a VSP experiment.

To obtain the desired expression of the P-wave phase velocity $v_p(p_x)$ in terms of the horizontal slowness, we use the exact formula

$$v_p^2(\theta) = \alpha_0^2\left[1 + \varepsilon \sin^2\theta - f(1 - \sqrt{s_\theta})/2\right], \tag{23}$$

with

$$s_\theta = 1 + \frac{4\sin^2\theta}{f}(2\delta\cos^2\theta - \varepsilon\cos(2\theta)) + \frac{4\varepsilon^2\sin^4\theta}{f^2}, \tag{24}$$

and θ the phase angle (Tsvankin, 1996). Using Snell's law ($\sin\theta = v_p p_x$) and rearranging terms produces the required expression $v_p(p_x)$:

$$v_p^2(p_x) = \frac{\alpha_0^2\left(2 - f + 2(\delta f - \varepsilon)p_x^2\alpha_0^2 + f\sqrt{s_p}\right)}{2 - 4\varepsilon p_x^2\alpha_0^2 - 4f(\varepsilon - \delta)p_x^4\alpha_0^4}, \tag{25}$$

with $f = 1 - \beta_0^2/\alpha_0^2$ and

$$s_p = 1 + 4\left(\frac{2\delta - \varepsilon}{f} - \delta\right)p_x^2\alpha_0^2 + 8 \times \left(\delta^2/2 + \delta - \varepsilon + \frac{\varepsilon - \delta - \delta\varepsilon}{f} + \frac{\varepsilon^2}{2f^2}\right)p_x^4\alpha_0^4. \tag{26}$$

For SV-waves, very similar expressions are involved. The sign in front of the square root in equations (23) and (25) is simply reversed. That is, the expressions change to

$$v_{sv}^2(\theta) = \alpha_0^2\left[1 + \varepsilon\sin^2\theta - f(1 + \sqrt{s_\theta})/2\right] \tag{27}$$

and

$$v_{sv}^2(p_x) = \frac{\alpha_0^2\left(2 - f + 2(\delta f - \varepsilon)p_x^2\alpha_0^2 - f\sqrt{s_p}\right)}{2 - 4\varepsilon p_x^2\alpha_0^2 - 4f(\varepsilon - \delta)p_x^4\alpha_0^4}. \tag{28}$$

The terms s_θ and s_p are again expressed by equations (24) and (26), respectively. It should be noted that expression (27) cannot handle multivalued SV-wave velocities for a single horizontal slowness. Such behavior can occur for strongly anomalous anisotropy ($\sigma \ll 0$), in which case a cusp lies near the horizontal axis.

Now that the phase velocity as a function of the horizontal slowness is known, a very simple procedure yields the exact moveout curves in the time domain by means of the τ-p transform (18). Namely, for a given slowness p_x, expressions (21) and (22) produce the exact intercept time τ. The required offset x is obtained from the local slope of the $\tau(p_x)$ curves. That is, $x = -d\tau/dp$, which follows directly from equation (18). Unfortunately, although $d\tau/dp$ can be calculated analytically, it is a rather involved expression for VTI media. Hence, we simply approximate it using finite differences (i.e., by means of a central differentiation). Therefore, exact moveout curves can be calculated for arbitrary anisotropy without the need of any Taylor series expansions or ray tracing.

Inversions: Parameter estimation

Equation (22) describing the form of the $\tau(p_x)$ curves can also be used for inversion purposes to estimate the anisotropy parameters. However, a strong nonuniqueness occurs in the inversion problem. A range of VTI anisotropy models exists which have very similar P- and SV-wave moveout curves, that is, they are kinematically equivalent.

For instance, Alkhalifah and Tsvankin (1995) demonstrated that the kinematic behavior of the P-wave moveout curves depends principally on the stack velocity α_n and the anisotropy parameter η. We therefore require an expression for the P-wave phase velocity $v_p(p_x)$ or its vertical slowness p_z which only depends on these two parameters.

Using an acoustic approximation (i.e., $\beta_0 = 0$), Alkhalifah (1998) derived a reduced-parameter expression for the vertical slowness p_z of the P-waves. His expression (A-10) is exactly equal to the squared normalised $\tau(p_x)$ curves [equation (22)]. That is,

$$\alpha_0^2 p_z^2 = 1 - \frac{p_x^2\alpha_n^2}{1 - 2\eta p_x^2\alpha_n^2} = \tau^2(p_x)/\tau_0^2. \tag{29}$$

Despite the acoustic approximation, expression (29) accurately predicts the exact $\tau(p_x)$ curves except when the vertical SV velocity β_0 becomes close to the vertical P-wave velocity α_0—a situation which is not very likely to occur.

Contrary to the exact case, the emergence offset x of the P-waves can easily be computed from the local slope of the reduced-parameter expression (29). However, we prefer to compute a finite-difference approximation for reasons of consistency.

A two-parameter approximation for the SV velocities can also be obtained. Namely, using the first-order approximation for v_{sv} (Thomsen, 1986),

$$v_{sv}^2(\theta) \approx \beta_0^2[1 + 2\sigma \cos^2\theta \sin^2\theta], \tag{30}$$

and applying Snell's law yields

$$v_{sv}^2(p_x) \approx \frac{-1 + 2\sigma p_x^2 \beta_0^2 + \left\{\left(1 - 2\sigma p_x^2\beta_0^2\right)^2 + 8\sigma p_x^4 \beta_0^4\right\}^{1/2}}{4\sigma p_x^4 \beta_0^2}, \tag{31}$$

with $\sigma = (\varepsilon - \delta)\alpha_0^2/\beta_0^2$. Expression (31) is a reasonably close approximation to the exact SV phase velocity except if large negative values of σ occur—in which case a wavefront cusp near the vertical axis may occur. Naturally, equation (31) can also be expressed in terms of the stack velocity β_n and σ using equation (3). However, $v_{0,i}$ in equation (22) remains equal to $\beta_{0,i}$ in this case. Note also that if the denominator approaches 0, then the SV-phase velocity converges to the vertical velocity β_0.

An inversion strategy now becomes straightforward. First, the seismic data is transformed to the τ-p domain using equation (18). Then, the semielliptical $\tau(p_x)$ curves are picked for several reflectors. Next, for each horizontal slowness value p_x, the differential intercept times $\Delta\tau_i = \tau_i - \tau_{i-1}$ are calculated for each layer [equation (21)]. This is the so-called layer-stripping operation. Finally, using a local or global inversion scheme and expression (22), the observed $\Delta\tau_i(p_x)$ curves are fitted layer by layer to retrieve the anisotropy parameters of each interval separately. The theoretical phase velocities are calculated using the two-parameter approximations (29) and (31) for P and SV-waves, respectively. Both the method for computing the traveltimes and the inversion procedure are demonstrated in more detail in the next section.

NUMERICAL EXAMPLES

To illustrate the numerous advantages of the τ-p transform both as a forward modeling and an inversion tool, we consider four different shales reported in Thomsen (1986). These shales are denoted by the letters A, B, C, and D, and are typical for both normal ($\eta, \sigma > 0$: shale A and B) and anomalous (η, $\sigma < 0$: shale C and D) anisotropy. Shales A and C can be considered as moderately anisotropic, whereas shales B and D are strongly anisotropic and display cusps in the SV-moveout curves. Table 1 contains their elastic parameters, and Figure 1 displays the associated phase slowness and group velocity surfaces.

Shales A and B are called normally anisotropic since they are the predominantly occurring type (Thomsen, 1986). Their SV phase-slowness surfaces have inflection points which causes either a kink or cusps near 45° in the group-velocity surface. In contrast, the inflection points in the slowness surfaces of the anomalous shales C and D produce either kinks (C) or cusps (D) in the group-velocity surfaces at both the horizontal and vertical axes (Figure 1).

Traveltimes and their inversion (single-layer model)

First, we consider the P and SV moveout curves of 1-km-thick packages of each shale. The exact moveout and $\tau(p_x)$ curves are displayed in Figure 2 as solid lines. The exact traveltimes (left column) were calculated using the τ-p transform (18), expression (22) describing the form of the $\tau(p_x)$ curves, the exact phase velocity expressions for P-waves (25) and SV-waves (28), and the relation $x = -d\tau/dp$. The exact $\tau(p_x)$ curves are also displayed (right column). All curves have been checked with those produced by the exact ray-tracer ATRAK (Guest and Kendall, 1993) and were found to be identical. Therefore, the new method can perfectly deal with arbitrarily strong VTI anisotropy and even kinks and cusps in the SV moveout curves for both normal and anomalous anisotropy. The abrupt termination of the $\tau(p_x)$ curve for shale D for SV-waves is caused by the fact that equation (28) cannot handle multiple-phase velocities for a single horizontal slowness. These phase velocities only affect reflection moveout curves of surface seismics for infinite offsets and, therefore, pose no problem.

Figure 2 also displays moveout and $\tau(p_x)$ curves of the two-parameter approximations for the P and SV phase velocities (long dashes). These curves have been obtained in a similar way as above except that the approximate equations (29) and (31) have been used instead of the exact phase velocity expressions. For P-wave data, the two-parameter expression (29) is highly accurate; its curves are indistinguishable from the exact curves. The acoustic approximation $\beta_0 = 0$ does not seem to affect accuracy. Unfortunately, the first-order approximation for the SV phase velocities (31) produces less accurate results. The strongly anomalous shale D produces the largest discrepancy. Nevertheless, both cusps and kinks are reproduced.

Finally, Figure 2 also shows the results of the Taylor series expansion (short dashes). The moveout curves have been obtained using expressions (7) and (8), and the $\tau(p_x)$ curves using expressions (7), (8), (12), and (13), and the τ-p transform (18). The Taylor series expansion yields quite accurate results for the P-wave moveout curves. However, predictions are less accurate than those of the two-parameter τ-p method. For instance, for shale B in the far offset ($x = 5$ km), errors of, respectively, 27 ms and 0.5 ms are produced for the Taylor series expansion and the two-parameter τ-p method. Errors become even larger in the case of many layers.

For SV-waves, the Taylor series method only yields good approximations for short and intermediate offsets ($x/z \le 1.5$)

Table 1. Elastic parameters of the shales used in the numerical examples. All values are from Thomsen (1986).

Symbol	Generic name	v_p (km/s)	v_s (km/s)	ε	δ	γ	η	σ	ρ (g/cm^3)
A	Taylor sandstone	3.368	1.829	0.110	−0.035	0.255	0.156	0.492	2.500
B	shale (5000)	3.048	1.490	0.255	−0.050	0.480	0.339	1.276	2.420
C	Mesaverde (4903) mudshale	4.529	2.703	0.034	0.211	0.046	−0.124	−0.497	2.520
D	Mesaverde (5501) clayshale	3.928	2.055	0.334	0.730	0.575	−0.161	−1.447	2.590

for normal anisotropy (A and B), i.e., up to the first kink or cusp. This is due to the fact that the quadratic and quartic coefficients have been approximated using the curvature near short offsets [equation (2)]. This can also be seen in the associated $\tau(p_x)$ curves. For the anomalous shales C and D, results are not useful as the kink/cusp affects the near offsets.

Similar conclusions can be drawn from inversion results. Table 2 reproduces estimates of the P-wave anisotropy parameters α_n and η obtained from both the Taylor series expansion and the τ-p method. Results were obtained using moveouts observed over a 5-km offset as measured in the x-t domain (Taylor series expansion) or τ-p domain (our method). In addition, Table 2 shows estimates for SV-wave anisotropy. The SV-wave parameters β_0 and σ have only been inverted using the τ-p method since the Taylor series expansion cannot handle kinks or cusps. Therefore, no useful results can be obtained with this method for long offsets. Table 2 clearly demonstrates that the τ-p method yields in all cases more robust and accurate results—even though the Taylor series expansion produces quite reliable estimates for the P-wave parameters.

It should be noted that, due to a strong nonuniqueness, we cannot invert for ε and δ separately using solely P or SV traveltime curves. Although a joint inversion might be a solution, the most effective method would incorporate well log information to retrieve α_0 and thereby ε and δ using expressions (3) and (6). Thomsen's (1986) remaining parameter γ can only be obtained if SH-waves are also recorded.

Therefore, the price we pay for rendering the inversion method more unique for P-wave data is that we cannot determine the depth to each reflector using pure-mode P-wave traveltimes solely. Only estimates of the stack velocity α_n and the anisotropy parameter η are obtained, whereas the anisotropy parameter δ is needed to compute the vertical P-wave velocity α_0. Therefore, no time-to-depth conversion can be undertaken. This theoretical drawback does not exist for pure-mode SV data since the inversion procedure directly produces the vertical SV-velocity β_0, which in combination with the zero-offset time yields the reflector depth.

Traveltimes and $\tau(p_x)$ curves for a multilayer model

Next, we consider a three-layer model which is composed of an isotropic layer ($\alpha = 2$ km/s, $\beta = 1$ km/s), a package of shale B, and again an isotropic layer ($\alpha = 4$ km/s, $\beta = 2$ km/s). Each layer has a thickness of 1 km. Figure 3 shows the moveout curves (left column) and the associated $\tau(p_x)$ curves (right column). All curves have been determined in a similar way as above except that effective values have been calculated for the Taylor

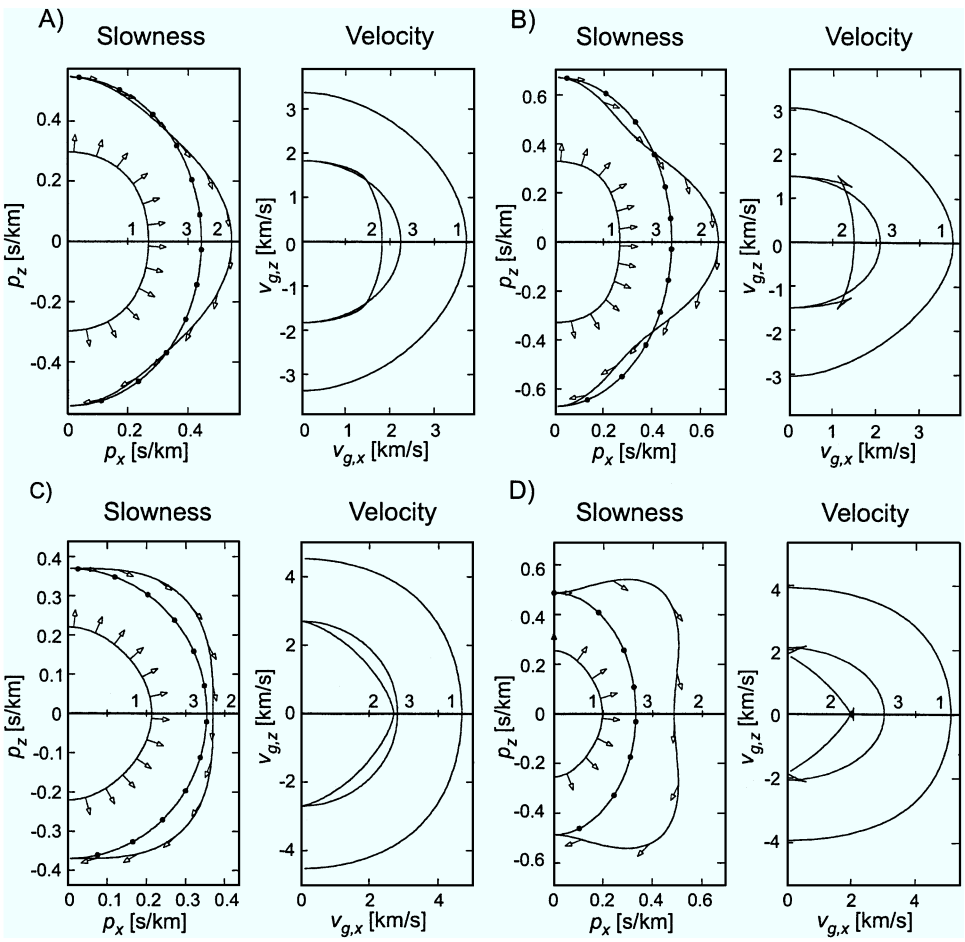

FIG. 1. Phase-slowness (left) and group-velocity (right) surfaces of the four shales A, B, C, and D considered in the numerical examples. Arrows indicate polarisations. Numbers $1 = P$, $2 = SV$, $3 = SH$. See Table 1 for the elastic coefficients.

series expansion [equations (9–11)]. Total intercept times τ are obtained using a simple summation over each individual layer [equation (21)].

Naturally, both the Taylor series expansion and the τ-p method using the two-parameter approximations for the phase velocities perfectly describe the moveout of the first isotropic layer. However, even for P-waves, the Taylor series expansion is not capable of accurately predicting the reflection moveouts of the second and third layer, whereas no such problems occur for the τ-p method using the two-parameter approximations. Its predictions are again indistinguishable from the exact P-wave curves. Also better results are obtained for the SV-waves.

Finally, it should be noted that, even though the third layer is isotropic, it is effectively anisotropic due to its overburden. This is most easily seen in its SV moveout curve, which displays

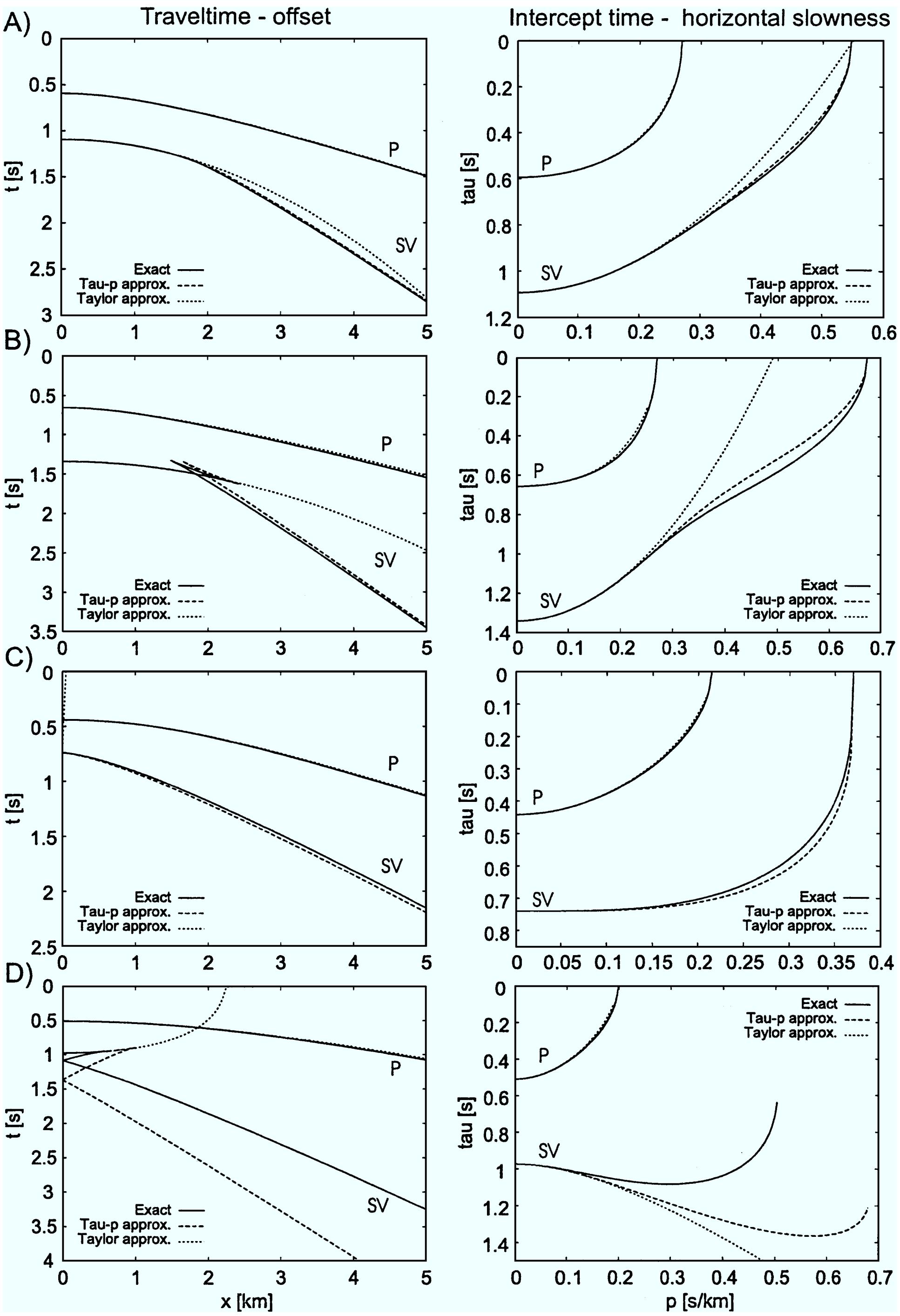

FIG. 2. Moveout (left) and $\tau(p_x)$ curves (right) associated with 1-km-thick packages of shales A, B, C, and D. Solid line: exact curves; long dashes: τ-p method using reduced-parameter expressions; short dashes: Taylor series approximation.

a kink at $x = 4.2$ km, and its $\tau(p_x)$ curve, which has a concave region instead of the expected ellipse.

In conclusion, Figures 2 and 3 clearly show that the two-parameter approximations for the phase velocities in combination with the τ-p transform produce much better results than the Taylor series expansion for both P- and SV-waves. It is especially noteworthy that the two-parameter approximation for the P-waves produces near-perfect results. In addition, for a stratified earth composed of homogeneous layers, the new method is capable of predicting the exact reflection moveout curves without the need of any ray tracing.

Layer stripping and multilayer inversions

The popular Taylor series expansion describes the perturbing influence of anisotropy on the reflection moveout in the time domain (e.g., Hake et al., 1984; Tsvankin and Thomsen, 1994). As a consequence, most inversion approaches are also performed in the x-t domain. However, as Figure 3b clearly shows, such an approach only yields effective estimates of the anisotropy. To invert for the local (interval) anisotropy, a layer-stripping method is needed in the time domain (Alkhalifah, 1997; Grechka and Tsvankin, 1998).

A similar procedure is applicable in the τ-p domain using expression (21). As a consequence, both effective and local estimates of the anisotropy parameters can be obtained. Figure 4 illustrates the technique using the exact $\tau(p_x)$ curves of the SV-waves of the three-layer model (right column in Figure 3b). Layer stripping in the τ-p domain corresponds to simply calculating the difference $\Delta\tau_i(p_x)$ between two adjacent $\tau(p_x)$ curves [equation (21)]. In this way, Figure 4b shows how the influence of the first isotropic layer and Figure 4c how the influence of the top two layers is removed. No a priori knowledge of depth or vertical slowness is required. For clarity, the stripped

Table 2. Inversion results for shales A, B, C, and D using both the Taylor series expansion and the τ-p method. Relative errors are indicated between parentheses. The Taylor series method cannot handle kinks and cusps in the SV-moveout curves. Therefore, no useful inversion results were obtained by this method.

	α_n (km/s)			η			β_0 (km/s)			σ		
Shale	Actual	Taylor	τ-p	Actual	Taylor	τ-p	Actual	Taylor	τ-p	Actual	Taylor	τ-p
A	3.248	3.228 (0.6)	3.244 (0.1)	0.156	0.153 (1.9)	0.157 (0.6)	1.829	—	1.808 (1.1)	0.492	—	0.502 (2.0)
B	2.892	2.839 (1.8)	2.890 (0.1)	0.339	0.318 (6.2)	0.336 (0.9)	1.490	—	1.450 (2.7)	1.276	—	1.267 (0.7)
C	5.401	5.340 (1.1)	5.366 (0.6)	−0.124	−0.127 (2.4)	−0.121 (2.4)	2.703	—	2.725 (0.8)	−0.497	—	−0.449 (9.7)
D	6.161	6.063 (1.6)	6.149 (0.2)	−0.161	−0.178 (10.6)	−0.171 (6.2)	2.055	—	1.984 (3.5)	−1.447	—	−0.928 (35.9)

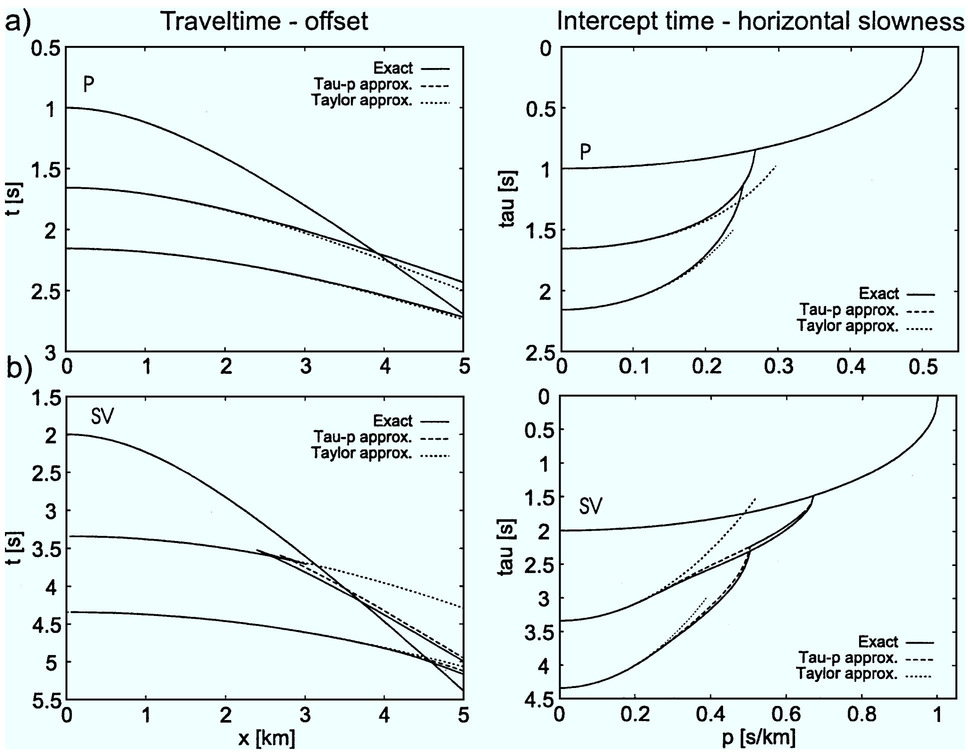

FIG. 3. Moveout and $\tau(p_x)$ curves of the three-layer model for (a) P-waves and (b) SV-waves. Only the second layer is anisotropic (shale B). Solid line: exact curves; long dashes: τ-p method using reduced-parameter expressions; short dashes: Taylor series approximation.

layers are plotted superposed on the zero-offset intercept time ($p_x = 0$) of the overburden.

After removal of the first isotropic layer, the moveout of the third (isotropic) layer remains effectively anisotropic since its $\tau(p_x)$ curve still has inflection points (Figure 4b). However, the $\tau(p_x)$ curve of the second layer has become identical to Figure 2b (right column), i.e., to the interval $\tau(p_x)$ curve of shale B. Similarly, after the removal of the overburden of the top two layers, it is evident that the last layer is isotropic since its $\tau(p_x)$ curve is perfectly elliptical.

Finally, we have also inverted the moveout curves of the three-layer model to obtain estimates of the interval parameters using again both methods. For the Taylor series method, the P-wave traveltime curves were inverted using a two-step procedure. First, the effective values were calculated. Then, the interval parameters are computed by explicitly expressing equations (9) and (10) in terms of the effective values of adjacent layers (Alkhalifah, 1997; Grechka and Tsvankin, 1998). The τ-p method, on the other hand, directly estimated the interval values using layer stripping. In addition, it also produced estimates of the SV-parameters. Results are contained in Tables 3 and 4. Again, the τ-p method produced more accurate results—especially for the second, anisotropic layer. Surprisingly, notwithstanding the large discrepancy in the analytically predicted and found η_{eff} for layer 2, the Taylor series method also predicted an isotropic third layer. This might be an indication that errors in estimates of the anisotropy parameters from the Taylor series method are proportional to the actual amount of anisotropy present. This is to a much lesser extent the case for the τ-p method.

An additional advantage of the τ-p method is that the influence of an overburden is simply removed by transforming the data to the τ-p domain, and picking and stripping the $\tau(p_x)$ curve of the unwanted overburden. Hence, the anisotropy in the target layers can directly be assessed without any further processing. Furthermore, applying an inverse τ-p transform to the stripped data results in an offset-time section where the influence of the horizontal anisotropic overburden has been removed, thereby allowing for conventional processing techniques to be used.

Table 3. Effective values for the *P*-wave moveout curves of the three-layer model as predicted and estimated by the Taylor series method.

	$\alpha_{n,eff}$ (km/s)		η_{eff}	
Layer	Analytical	Found	Analytical	Found
1 (isotropic)	2.000	2.000 (0.0)	0.000	0.000 (–)
2 (anisotropic)	2.393	2.382 (0.5)	0.196	0.298 (52.0)
3 (isotropic)	2.848	2.843 (0.2)	0.106	0.163 (53.8)

PRACTICAL CONSIDERATIONS FOR ANISOTROPY ESTIMATION

Nonhyperbolic moveout only occurs in the far offset (i.e., for ratios x/z greater than 1.5). As a matter of fact, offsets need to be at least 2–2.5 times the depth of the considered reflector before any confidence in the inversion results can be gained (Alkhalifah, 1997). This is a theoretical limitation which holds regardless whether Taylor-series expansions or τ-p methods are used. Therefore, high-quality data are needed to pick traveltimes or $\tau(p_x)$ curves to such offsets.

The required $\tau(p_x)$ curves can either be obtained from the τ-p transformed gathers or from picked traveltimes. Namely, the horizontal slowness can be computed from the differential moveout between receivers ($p_x = \partial t/\partial x$) and the τ-p transform (18). Furthermore, an interactive procedure can be applied in which picked curves are transformed to the other domain and overlain on the (transformed) data in

Table 4. Inversion results for the interval values of the three-layer model. Relative errors are indicated between parentheses. Again, no useful results could be obtained for the *SV*-parameters by the Taylor method.

	$\alpha_{n,i}$ (km/s)			η_i			$\beta_{0,i}$ (km/s)			σ_i		
Layer	Actual	Taylor	τ-p	Actual	Taylor	τ-p	Actual	Taylor	τ-p	Actual	Taylor	τ-p
1 (isotropic)	2.000	2.000 (0.0)	2.000 (0.0)	0.000	0.000 (–)	0.000 (–)	1.000	—	1.000 (0.0)	0.000	—	0.000 (–)
2 (anisotropic)	2.982	2.868 (3.8)	2.889 (3.1)	0.339	0.519 (53.1)	0.336 (0.9)	1.490	—	1.447 (2.9)	1.276	—	1.277 (0.1)
3 (isotropic)	4.000	4.008 (0.2)	4.000 (0.0)	0.000	0.005 (–)	0.000 (–)	2.000	—	2.000 (0.0)	0.000	—	0.000 (–)

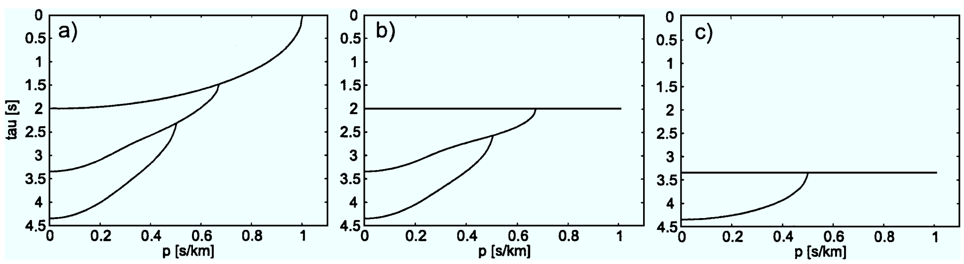

FIG. 4. Layer stripping in the τ-p domain: (a) $\tau(p_x)$ curves of all three SV-waves [identical to the exact curves in Figure 3b (right column)], (b) first layer removed, and (c) top two layers removed.

order to adapt and improve the picks. This strategy may be advantageous since noise in the x-t and τ-p domains displays different characteristics.

If the data do not allow for the picking of long-offset traveltimes, a three-parameter semblance analysis can be considered. This may in particular be an option for SV-data, since they display in general a lower signal-to-noise ratio than P-waves. However, beyond the point of critical reflection, a gradual phase shift occurs for all pure-mode phases. Furthermore, SV-waves may even display precritical polarity reversals. Such polarity reversals will degrade the performance of the semblance analysis, because it cannot handle phase changes. Hence, semblance as a coherency measure may not be an optimal choice.

Naturally, the available offset-to-depth ratio diminishes for deeper horizons. Resolution of anisotropy parameters decreases, therefore, with depth. Furthermore, the thickness of each horizon also affects resolution since the traveltime and $\tau(p_x)$ curves are scaled with the zero-offset times. Hence, the local properties of a thin layer are harder to estimate than those of a thicker interval. In the case of closely spaced reflections, we recommend using larger intervals comprised of a number of reflections.

Finally, the method assumes that the region is composed of laterally homogeneous layers. It can be shown that vertical gradients only slightly affect the estimation of anisotropy parameters (Hake, 1986; Alkhalifah, 1997). However, numerical simulations show that a large trade-off exists between lateral changes in the velocity and the obtained estimates for the anisotropy parameters. Hence, care has to be taken when applying the inversion method in regions which are known to be strongly heterogeneous. In such areas, it may be very difficult to obtain confident estimates of the actual anisotropy parameters.

DISCUSSION AND CONCLUSIONS

In this paper, we have presented a new method to calculate exact traveltimes of reflected P- and SV-waves and to solve the inverse problem for stratified, laterally homogeneous, anisotropic media using the τ-p transform without the need of any ray tracing. However, the principal relation describing the form of the $\tau(p_x)$ curves, equation (22), is only valid for pure-mode phases and anisotropy systems displaying a horizontal symmetry plane (like VTI, HTI, and orthorhombic media with a symmetry axis parallel to the z-axis). Fortunately, formula (22) is easily generalised to more complicated anisotropy systems (with, e.g., tilted symmetry axes). In that case, we have to deal with two one-way intercept times: one for the downgoing and one for the upgoing wave.

Equation (22) can also be used as an inversion tool to estimate the anisotropy parameters, namely α_n, η, β_0, and σ. Results have a higher accuracy than the Taylor series expansion (Tsvankin and Thomsen, 1994). Moreover, it can handle both cusps and kinks in the SV-wave moveout curves. Furthermore, a layer-stripping procedure can be applied such that both effective (average) and local (interval) estimates can be obtained. Unfortunately, inverting for anisotropy parameters is a rather nonunique process since a variety of anisotropic media may exhibit identical moveout. As a consequence, a reduction of the total number of parameters is required. This can be done by searching for parameters describing kinematically equivalent models [such as the η parameter in equation (29)] or by applying first-order approximations of the phase velocities only [such as the σ parameter in equation (31)]. The first approach is preferable. For the latter case, many useful expressions are published in Mensch and Rasolofosaon (1997) and Pšenčík and Gajewski (1998).

Unfortunately, due to the reduction of the number of parameters involved, the vertical P-wave velocity cannot be assessed using P-wave moveout only, and no time-to-depth conversion is possible without well log information. On the other hand, this drawback does not exist for pure-mode SV-data. The vertical SV-wave velocity is provided by the inversion method. This may be a further reason to advocate the acquisition of pure-mode shear-wave data for exploration purposes. However, SV-waves can suffer from poor signal-to-noise ratios and phase reversals, the effects of which on parameter estimation will need to be addressed.

We are presently extending the method to handle more generally anisotropic media (e.g., HTI), P-SV converted waves (including their conversion points), and laterally inhomogeneous media with, for example, fluctuating background velocities or varying quantities of anisotropy. The first two items are the topic of a forthcoming publication. Finally, we are also applying the new technique to real data.

ACKNOWLEDGMENTS

M.v.d.B. thanks Shell Expro UK for financial support. We also gratefully acknowledge the comments and suggestions of Tariq Alkhalifah, José Carcione, Jim Gaiser, Reinaldo Michelena, and an anonymous reviewer. We are also thankful to Tariq for referring to his acoustic approximation for the vertical P-wave slowness. This particular approximation was a further simplification of a formula we had derived without prior knowledge of his expression. Finally, we thank Dirk Smit for initiating the project and his continued support and feedback.

REFERENCES

Alkhalifah, T., 1997, Velocity analysis using nonhyperbolic moveout in transversely isotropic media: Geophysics, **62**, 1839–1854.
——— 1998, Acoustic approximations for processing in transversely isotropic media: Geophysics, **63**, 623–631.
Alkhalifah, T., and Tsvankin, I., 1995, Velocity analysis for transversely isotropic media: Geophysics, **60**, 1550–1566.
Banik, N. C., 1984, Velocity estimation of shales and depth estimation in the North Sea Basin: Geophysics, **49**, 1411–1419.
——— 1987, An effective parameter in transversely isotropic media: Geophysics, **52**, 1654–1664.
Berge, P. A., 1991, Estimating SV-wave stacking velocities for transversely isotropic solids: Geophysics, **56**, 1596–1602.
Gaiser, J. E., 1990, Transversely isotropic phase velocity analysis from slowness estimates: J. Geophys. Res., **95**, 11 241–11 254.
Grechka, V., and Tsvankin, I., 1998, Feasibility of nonhyperbolic moveout inversion in transversely isotropic media: Geophysics, **63**, 957–969.
Guest, W. S., and Kendall, J.-M., 1993, Modelling seismic waveforms in anisotropic inhomogeneous media using ray and Maslov asymptotic theory: Applications to exploration seismology: Can. J. Expl. Geophys., **29**, 78–92.
Hake, H., 1986, Slant stacking and its significance for anisotropy: Geophys. Prospect., **34**, 595–608.
Hake, H., Helbig, K., and Mesdag, C. S., 1984, Three-term Taylor series for t^2-x^2 curves over layered transversely isotropic ground: Geophys. Prospect., **32**, 828–850.

Kebaili, A., and Schmitt, D. R., 1996, Velocity anisotropy observed in wellbore seismic arrivals: Combined effects of intrinsic properties and layering: Geophysics, **61**, 12–20.
Mensch, T., and Rasolofosaon, P., 1997, Elastic wave velocities in anisotropic media of arbitrary anisotropy—Generalization of Thomsen's parameters ϵ, δ and γ: Geophys. J. Internat., **128**, 43–64.
Musgrave, M. J. P., 1970, Crystal acoustics: Introduction to the study of elastic waves and vibrations in crystals: Holden-Day.
Pšenčík, I., and Gajewski, D., 1998, Polarization, phase velocity, and NMO velocity of qP-waves in arbitrary weakly anisotropic media: Geophysics, **63**, 1754–1766.
Schmitt, D. R., and Kebaili, A., 1993, Velocity anisotropy estimation from slant stacks of wellbore seismics: Can. J. Expl. Geophys., **29**, 236–245.
Schultz, P. S., 1982, A method for direct estimation of interval velocities: Geophysics, **47**, 1657–1671.
Taner, M. T., and Koehler, F., 1969, Velocity spectra-digital computer derivation and applications of velocity functions: Geophysics, **34**, 859–881.
Thomsen, L., 1986, Weak anisotropy: Geophysics, **51**, 1954–1966.
Tsvankin, I., 1996, P-wave signatures and notation for transversely isotropic media: An overview: Geophysics, **61**, 467–483.
——— 1997, Anisotropic parameters and P-wave velocity for orthorhombic media: Geophysics, **62**, 1292–1309.
Tsvankin, I., and Thomsen, L., 1994, Nonhyperbolic reflection moveout in anisotropic media: Geophysics, **59**, 1290–1304.
Vlaar, N. J., 1968, Ray theory for an anisotropic inhomogeneous elastic medium: Bull. Seism. Soc. Am., **58**, 2053–2072.
Winterstein, D. F., 1986, Anisotropy effects in P-wave and SH-wave stacking velocities contain information in lithology: Geophysics, **51**, 661–672.